



# Preparation of hexagonal and amorphous chromium oxyhydroxides by facile hydrolysis of $K_xCrO_y$

Shu-ting LIANG<sup>1,2</sup>, Hong-ling ZHANG<sup>3,4</sup>, Hong-bin XU<sup>3,4</sup>

1. College of Chemistry and Environmental Engineering, Chongqing University of Arts and Sciences, Chongqing 402160, China;
2. Chongqing Key Laboratory of Environmental Materials and Remediation Technologies, Chongqing University of Arts and Sciences, Chongqing 402160, China;
3. National Engineering Laboratory for Hydrometallurgical Cleaner Production Technology, Institute of Process Engineering, Chinese Academy of Science, Beijing 100190, China;
4. Key Laboratory of Green Process and Engineering, Institute of Process Engineering, Chinese Academy of Sciences, Beijing 100190, China

Received 9 June 2019; accepted 30 March 2020

**Abstract:** The hydrolysis process and mechanisms of unique as-prepared  $KCrO_2$  and  $K_3CrO_4$  were systematically investigated. The characterization results of XRD, IR and SEM show that the hydrolysis reaction can be realized at a low reaction temperature of 80 °C and a reaction time of 24 h. Moreover, the greyish-green  $\alpha$ -CrOOH with a hexagonal plate-like morphology and a large size of 10  $\mu\text{m}$  is formed via the hydrolysis of the single-phase hexagonal  $KCrO_2$ , while the green sol-gel of amorphous  $Cr(OH)_3$  with a lumpy aggregate morphology is generated through the hydrolysis of a cubic  $K_3CrO_4$ . It is a facile and rapid method to synthesize pure-phase chromium oxyhydroxide via the above hydrolysis.

**Key words:** hydrolysis process; CrOOH; chromium oxide; activated  $K_xCrO_y$ ; reaction mechanism

## 1 Introduction

Hydrous chromium oxides ( $Cr_2O_3 \cdot xH_2O$ ) such as chromium hydroxide ( $Cr(OH)_3$ ) and chromium oxyhydroxide (CrOOH) offer a near-ideal combination of distinctive adsorption selectivity and magnetic properties. The remarkable CrOOH and  $Cr(OH)_3$  have piqued the interest of many researchers as a consequence of their potential applications as catalysts [1], colorants, fluorescent and magnetic bifunctional molecules [2–5]. The chromium oxide ( $Cr_2O_3$ ) was also generated from

thermal decomposition of CrOOH or  $Cr(OH)_3$  [3,6], and it was important in applications such as catalysts [7], functional pigments [8–11], hydrogen storage [12], gas sensors [13], batteries [14] or electrode [15], and metallic ferromagnetic material [16–18].

Nowadays, rhombohedral chromium oxyhydroxide ( $\alpha$ -CrOOH) has been mostly prepared via the hydrothermal reaction of  $Cr(NO_3)_3 \cdot 9H_2O$  [19–22]. The  $\alpha$ -CrOOH with different diameters [23], morphologies [24], adsorption properties [25] and catalytic properties has been prepared through the hydrothermal method. Based on the hydrothermal

**Foundation item:** Project (R2018SCH02) supported by the High-level Talents Foundation of Chongqing University of Art and Sciences, China; Project (P2018CH10) supported by Major Cultivation Program of Chongqing University of Arts and Sciences, China; Project (cstc2019jcyj-msxmX0788) supported by the Natural Science Foundation of Chongqing, China; Project (KJQN201901342) supported by the Science and Technology Research Program of Chongqing Municipal Education Commission, China

**Corresponding author:** Shu-ting LIANG; Tel: +86-23-61162725; E-mail: [stliang@mail.tsinghua.edu.cn](mailto:stliang@mail.tsinghua.edu.cn)

DOI: 10.1016/S1003-6326(20)65305-5

technique developed [18,19], the  $\alpha$ -CrOOH was produced with a size of 10–300 nm. By controlling the synthetic parameters, especially the temperature and pH, the crystallinity of the final products would be greatly influenced [26]. This same hydrothermal reduction of chromate has already been experimentally applied to preparing Cr(OH)<sub>3</sub>, which was performed in a sealed autoclave to control the atmospheric pressure.

However, in the previous work, the high reaction pressure and temperature, complex process control, and unable monitoring of CrOOH during the crystal-growing process have been widely considered as the weakness. Unfortunately, as one of the crystallographically well-defined K<sub>x</sub>CrO<sub>y</sub> compounds, KCrO<sub>2</sub> and K<sub>3</sub>CrO<sub>4</sub> were extremely sensitive to moisture and oxygen [27]. They were very difficult to prepare and preserve in the air [28]. In particular, few studies have reported the reactions of KCrO<sub>2</sub> and K<sub>3</sub>CrO<sub>4</sub> compounds with water over the past few years.

In this current work, rhombohedral  $\alpha$ -CrOOH and amorphous Cr(OH)<sub>3</sub> were synthesized via a low-temperature and stress-free process, rather than the traditional preparation method. This alternative techniques could effectively reduce the high reaction temperature and pressure, save the reaction energy consumption, and also optimize the control and monitoring of products in the reaction process. In parallel with this, a new technical concept of hydrolysis of K<sub>x</sub>CrO<sub>y</sub> compounds was proposed, and the hydrolysis processes of KCrO<sub>2</sub> and K<sub>3</sub>CrO<sub>4</sub> were accidentally discovered, and a series of  $\alpha$ -CrOOH and Cr(OH)<sub>3</sub> were produced using this hydrolysis reaction. The hydrolysis processes of KCrO<sub>2</sub> and K<sub>3</sub>CrO<sub>4</sub> were performed in an inert atmosphere for the sake of preventing their oxidation. The crystal structures, chemical compositions, morphological characteristics, and sizes of hydrolysates ( $\alpha$ -CrOOH and Cr(OH)<sub>3</sub>) were described in more detail. Finally, the formation mechanisms of  $\alpha$ -CrOOH and Cr(OH)<sub>3</sub> were deeply proposed, respectively.

## 2 Experimental

99.5% purity potassium chromate (K<sub>2</sub>CrO<sub>4</sub>) was purchased from Sinopharm Chemical Reagent Co., Ltd., and used to produce KCrO<sub>2</sub> and K<sub>3</sub>CrO<sub>4</sub> [29,30]. 99.99% purity hydrogen gas was

purchased from Praxair Inc.. KCrO<sub>2</sub> and K<sub>3</sub>CrO<sub>4</sub> were produced via hydrogen reduction, which was reported in previous papers [29,30]. KCrO<sub>2</sub> used in this work was obtained via hydrogen reduction of K<sub>2</sub>CrO<sub>4</sub> at 650 °C for 2 h; while K<sub>3</sub>CrO<sub>4</sub> was also obtained via hydrogen reduction of K<sub>2</sub>CrO<sub>4</sub> at 450 °C for 0.5 h. A nickel boat, loaded with 5 g of K<sub>2</sub>CrO<sub>4</sub>, was placed into the furnace tube. Hydrogen was introduced into the tube at a flow rate of 0.6 L/min. After the reduction reaction was finished, different reduction products such as KCrO<sub>2</sub> and K<sub>3</sub>CrO<sub>4</sub> were added to distilled water immediately, which were maintained constant stirring for more than 24 h at 80 °C. Some greyish-green powdery substances observed in the solution were separated through centrifugation and dried at 100 °C for 12 h.

X-ray diffraction (XRD) patterns were recorded using a Rigaku diffractometer employing Cu K $\alpha$  radiation. The infrared spectrum was recorded using a Spectro GX FT-IR spectrometer (Perkin-Elmer, USA) in KBr pellets. The morphological characteristic was performed using a JSM-6700F NT scanning electron microscopy (SEM), supplied by Japan. The transmission electron microscopy (TEM), selected area electron diffraction (SAED) and energy dispersive spectroscopy (EDX) were taken with a JEOLJEM 2010 operating at an acceleration voltage of 200 kV.

## 3 Results and discussion

### 3.1 Characterization of KCrO<sub>2</sub>

Using a facile and highly reproducible hydrogen reduction method, KCrO<sub>2</sub> was prepared at 650 °C. As shown in Fig. 1(a), the XRD patterns of the synthesized precursor, show that all diffraction peaks can be indexed to the KCrO<sub>2</sub> with a rhombohedral crystal structure, indicating that the precursor has a single crystalline phase. The lattice constants of the precursor obtained via the refinement of XRD data were  $a=0.3022$  nm and  $c=1.7760$  nm, which was consistent with the potassium chromate (KCrO<sub>2</sub>, JCPDS No. 28-0743). According to Ref. [6], KCrO<sub>2</sub> was a green powder with a magnetic property, and it was extremely sensitive to moisture and oxygen as well. In the previous work, KCrO<sub>2</sub> has been synthesized via an azide route or a nitrate route [26–28], which must be executed at a high temperature and dangerous

pressure. Notably,  $\text{KCrO}_2$  could be prepared by hydrogen reduction of  $\text{K}_2\text{CrO}_4$  in this work, which was more pressure-free and clean.

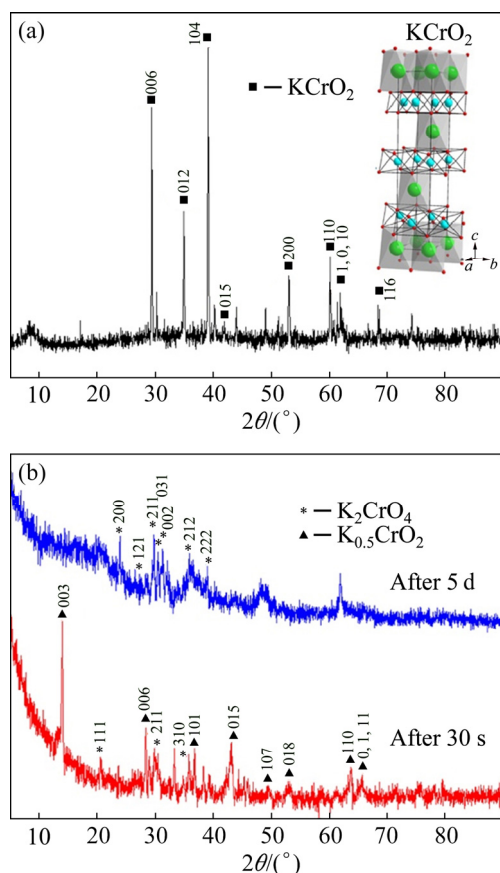


**Fig. 1** XRD patterns of  $\text{KCrO}_2$  and crystal structure of  $\text{KCrO}_2$  (K (green spheres), Cr (blue spheres) and O (red spheres)) (a) and XRD patterns of oxidation products of  $\text{KCrO}_2$  in air at room temperature after 30 s and 5 d (b)

The oxidation reaction of  $\text{KCrO}_2$  occurred naturally at room temperature in air. The behavior of  $\text{KCrO}_2$  during oxidation with air was discussed. Figure 1(b) shows the XRD results for the oxidation of  $\text{KCrO}_2$ . After exposing in air for 30 s, the  $\text{KCrO}_2$  was converted to a mixture of  $\text{K}_{0.5}\text{CrO}_2$  and  $\text{K}_2\text{CrO}_4$ . It has been also reported that  $\text{KCrO}_2$  was immediately oxidized and yielded a mixture of  $\text{K}_{0.5}\text{CrO}_2$  and  $\text{K}_2\text{CrO}_4$  at room temperature in the air [27]. The conversion rate from  $\text{KCrO}_2$  to  $\text{K}_{0.5}\text{CrO}_2$  was not 100% at room temperature. As illustrated in Fig. 1(b), the reduction product after exposing in air for 30 s contained a mixture of  $\text{K}_{0.5}\text{CrO}_2$  (PDF No.00–28–0745), and  $\text{K}_2\text{CrO}_4$  (PDF No. 00–15–0365).

The phase transition from  $\text{K}_{0.5}\text{CrO}_2$  to  $\text{K}_2\text{CrO}_4$  was observed as well, and the complete conversion took place after 5 d in air. Therefore, in an

atmosphere of air, the most likely process was the conversion of  $\text{KCrO}_2$  to  $\text{K}_{0.5}\text{CrO}_2$  and then the conversion of  $\text{K}_{0.5}\text{CrO}_2$  to  $\text{K}_2\text{CrO}_4$ . Hence, it is very important to control the oxygen level at as low a level as possible in the next following hydrolysis process.

### 3.2 Hydrolysis of $\text{KCrO}_2$ to prepare $\alpha\text{-CrOOH}$

Considering the easy oxidation of  $\text{KCrO}_2$ ,  $\text{KCrO}_2$  was cooled naturally to ambient temperature in an inert atmosphere. In the next,  $\text{KCrO}_2$  (2 g) was immediately added to the 100 mL distilled water for analyzing the hydrolysis process.

An overview of the hydrolysis taken in this work is presented in Fig. 2(a). This material was

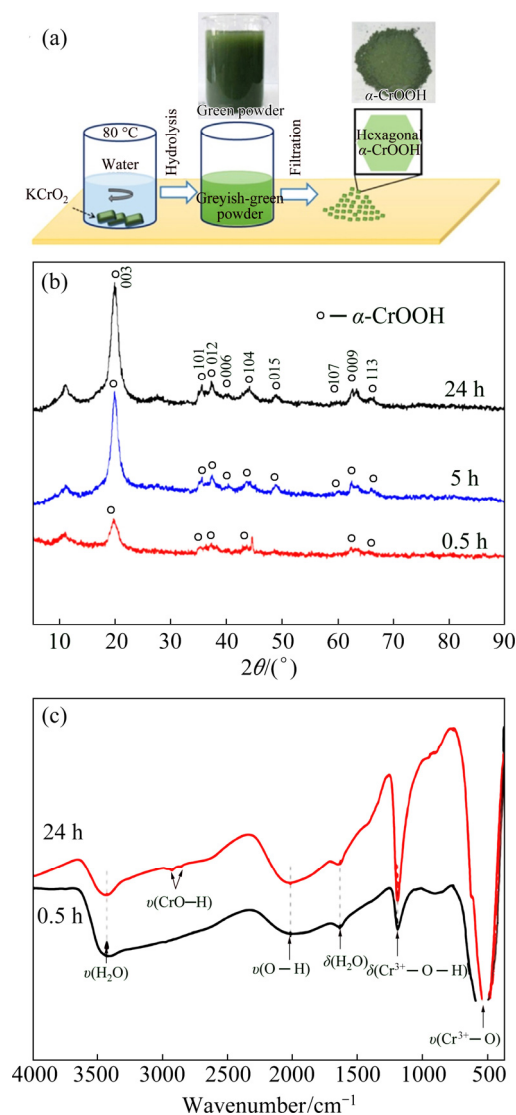


**Fig. 2** Schematic diagram of hydrolysis process of  $\text{KCrO}_2$  and photograph of greyish-green hydrolysis product of  $\text{KCrO}_2$  (a), XRD patterns of hydrolysis products treated at 80 °C for 0.5, 5, 24 h (b) and FT-IR spectra of hydrolysis products treated for 24 and 0.5 h (c)

vigorously stirred at 80 °C for 24 h. After mild hydrolysis of  $\text{KCrO}_2$ , quite a few greyish-green powdered substances were observed in the solution. This remaining solid-green powder was separated by centrifugation and then dried at 100 °C for 12 h. The hydrolysis process of different reduction products would be analyzed.

Different greyish-green powdered materials were formed through the hydrolysis of  $\text{KCrO}_2$  for different durations of 0.5, 5, and 24 h at 80 °C. As shown in Fig. 2(b), all the patterns observed from hydrolysis product showed the characteristic diffraction peaks of  $\alpha$ -CrOOH with a rhombohedral crystal structure (space group of  $R\bar{3}m$ ), and lattice constants of  $a=0.2984$  nm and  $c=1.34$  nm, and all the peaks were in good agreement with the JCPDF No. 09–0331 [23]. From Fig. 2(b), hydrolysis duration could be deduced to have a great influence on the crystallization of  $\alpha$ -CrOOH. The XRD peaks of the sample treated for 0.5 h were weak and broad (as shown in red line), indicating that the structure has poor degree of crystallization. Furthermore, hydrolysate after 24 h shows increase in all peak intensities (as shown in black line). The results suggest that the nucleation and growth of  $\alpha$ -CrOOH crystallites could be accelerated by a longer hydrolysis duration.

The FT-IR absorption spectrum in Fig. 2(c) clearly demonstrated that samples treated for 24 h and 0.5 h showed five bands: 3247, 2017, 1635, 1190 and 599  $\text{cm}^{-1}$ . The strong sharp peak at 599  $\text{cm}^{-1}$  corresponded to the  $\text{Cr}^{3+}-\text{O}$  anti-symmetric stretching vibration [23]. Another strong sharp peak at 1190  $\text{cm}^{-1}$  was assigned to  $\text{Cr}^{3+}-\text{O}-\text{H}$  bending vibration [31]. A low-intensity band observed at 1635  $\text{cm}^{-1}$  corresponded to the bending modes of non-dissociated water molecules [32]. The appearance of a broadband in the 1700–2100  $\text{cm}^{-1}$  region was assigned to the  $\text{O}-\text{H}$  stretching vibration in the OH group of CrOOH [33]. While the other broadband in the 2800–3500  $\text{cm}^{-1}$  region was assigned to the surface OH stretching groups originated from dissociation chemisorptions of water [34,35]. Table 1 lists the summary of FT-IR bands and their assignments of the hydrolysate. These bands were characteristics of

$\alpha$ -CrOOH, which further indicated that the hydrolysis product was composed of  $\alpha$ -CrOOH with a rhombohedral crystal structure.

A few representative SEM and TEM images were provided, which were used to determine the final morphology of the product after 24 h of hydrolysis. As shown in Fig. 3(a), the morphology of hydrolysate after treating for 24 h was hexagonal plate-like particles with a diameter of 10  $\mu\text{m}$ .

A more complete set of SAED pattern as well as EDX mapping from the analyzed sample treated for 24 h was available in Figs. 3(b, c). The hexagonal single crystal particle of  $\alpha$ -CrOOH gave a well-defined sixfold symmetric electron diffraction pattern, as shown in Fig. 3(b), confirming the existence of the crystalline structure of rhombohedral  $\alpha$ -CrOOH. In the meanwhile, the selected area electron diffraction pattern of the hexagonal single crystal particle took along the  $[\bar{1}11]$  zone axis. As shown in the SAED patterns of Fig. 3(c), diffraction points, which were recorded from the  $\alpha$ -CrOOH, could be identified as (101), (110), and (202) planes of the  $\alpha$ -CrOOH. The corresponding EDS spectrum (Fig. 3(d)) highlighted the presence of only chromium, oxygen and potassium peaks. In addition, Cu and C could also be observed, which was attributed to the copper TEM sample copper grids and carbon film. In this research, oversize particle (10  $\mu\text{m}$ ) was obtained successfully via the hydrolysis technique.

### 3.3 Characterization of $\text{K}_3\text{CrO}_4$

In the previous work,  $\text{Cr}_2\text{O}_3$ , KOH, and  $\text{K}_2\text{CrO}_4$  were used as the raw materials for the typical route to synthesize  $\text{K}_3\text{CrO}_4$ , and the reaction was completed at 700 °C for approximately 8 h [24,25]. The dark-green  $\text{K}_3\text{CrO}_4$  was also highly hygroscopic and sensitive, and it was spontaneous oxidation at room temperature. Various researchers have suggested that the oxidation state of  $\text{Cr}^{5+}$  was rather unstable. In this work,  $\text{K}_3\text{CrO}_4$  was prepared through a simple low-temperature hydrogen reduction method. The XRD pattern of the prepared product is presented in Fig. 4(a) for crystal phase identification. It was obvious that the main lines were the diffraction peaks of the crystallized cubic

**Table 1** FT-IR bands and assignments of hydrolysates ( $\text{cm}^{-1}$ )

$\text{Cr}^{3+}-\text{O}$ stretching	$\text{Cr}^{3+}-\text{O}-\text{H}$ bending	Water $\text{H}-\text{O}-\text{H}$ bending	$\text{H}-\text{O}-\text{H}$ stretching	$\text{H}_2\text{O}$ stretching
599	1190	1635	2017	3247

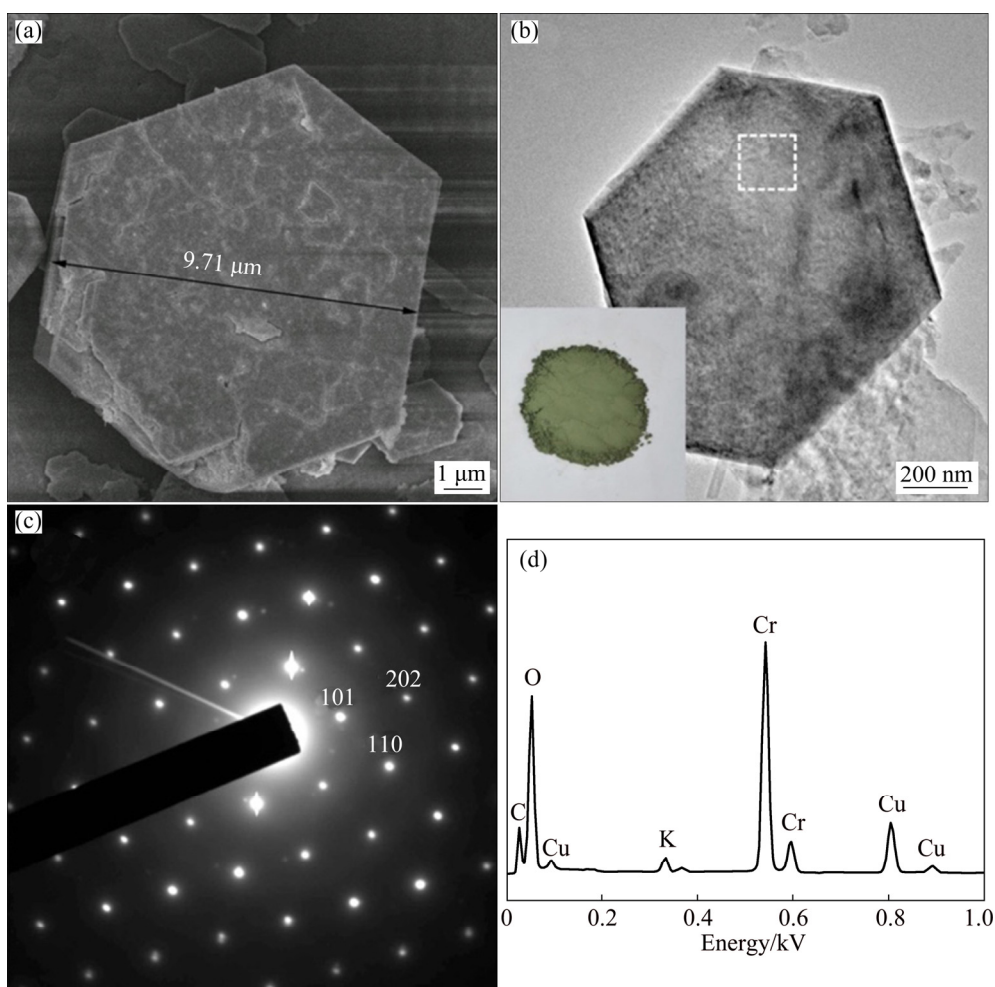


**Fig. 3** SEM image (a), TEM image (b), SAED pattern (c) and EDX mapping (d) of hydrolysates (The location of the examined area of SAED pattern and EDX mapping is indicated in (b) with a frame. The region in the inset of (b) shows the photograph of the greyish-green powdered  $\alpha$ -CrOOH)

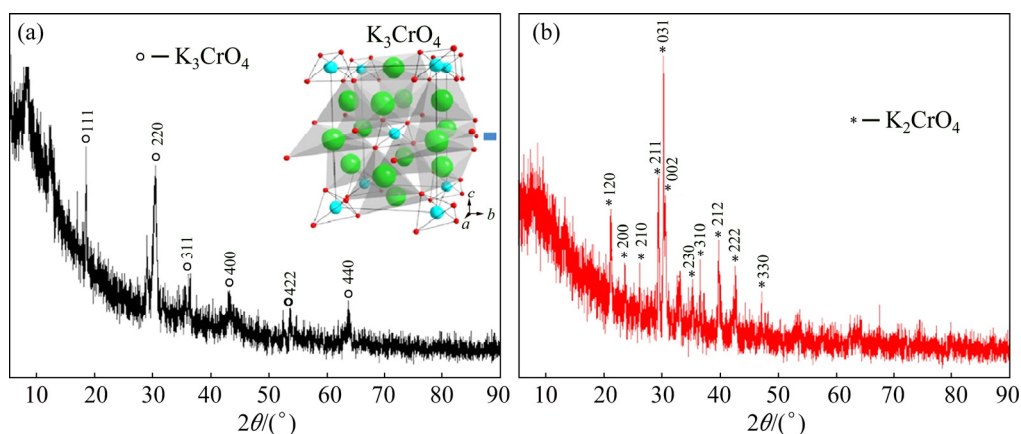


**Fig. 4** XRD pattern of  $K_3CrO_4$  and its crystal structure (K (green spheres), Cr (blue spheres), O (red spheres)) (a) and XRD pattern of oxidation product of  $K_3CrO_4$  in air for 24 h at room temperature (b)

$K_3CrO_4$  (lattice constants  $a=b=c=0.83368$  nm, PDF No. 00–31–0994).

Figure 4(b) shows the XRD results for the oxidation of  $K_3CrO_4$  in air at room temperature. It

can be seen that the oxidation of  $K_3CrO_4$  was an easy process in air. It was observed that the diffraction peak for  $K_3CrO_4$  completely disappeared, whereas the diffraction peak for  $K_2CrO_4$  appeared.

The presence of air significantly promoted the  $K_3CrO_4$  oxidation. After exposing the  $K_3CrO_4$  and  $K_2CrO_4$  system in air for 24 h, only the  $K_2CrO_4$  remained.

### 3.4 Hydrolysis of $K_3CrO_4$ for preparing $Cr(OH)_3$

The hydrolysis process of  $K_3CrO_4$  was performed in an inert atmosphere for the sake of preventing its oxidation. After the hydrolysis of  $K_3CrO_4$ , several green flocculent substances were observed in the solution. Interestingly, when the solution was completely placed and heated at  $60\text{ }^\circ\text{C}$  for 2 h, a type of green sol-gel material was precipitated. The color of the solution was changed from green to yellow, which indicated that  $Cr^{6+}$  was generated. This obtained green gel-like precipitate was centrifuged at 10000 r/min for 10 min and washed three times with distilled water, as shown in Fig. 5(a). Figure 5(b) shows the XRD pattern of the green gel-like precipitate sample prepared by hydrolysis treatment for 0.5 and 24 h, all the hydrolysates presented an amorphous phase, which

indicated that it was impossible to directly characterize the hydrolysates in this experiment.

To further understand the main component of the hydrolysis product of  $K_3CrO_4$ , the FT-IR absorption data were evaluated. The FT-IR absorption spectrum was collected and plotted in Fig. 5(c). As observed, the  $540\text{ cm}^{-1}$  broadband corresponded to  $Cr^{3+}-O$  lattice vibrations; at  $919\text{ cm}^{-1}$ , the peak corresponded to the bending vibration of  $Cr^{3+}-O-H$  [31]. While three absorption peaks of  $Cr(OH)_3$  at 1377, 1497, and  $1634\text{ cm}^{-1}$  [30], can also be observed in the spectra. The result indicated that the gel-like precipitate contained  $Cr(OH)_3$ , which was directly generated by the hydrolyzing process of  $K_3CrO_4$  in this system.

Transmission electron microscopy (TEM) was used to investigate the final morphology and crystallographic properties of the  $Cr(OH)_3$  product. TEM analysis revealed that the surface of  $Cr(OH)_3$  product was relatively rough, lumpy, and irregular in Fig. 6(a). The SAED spectrum also strongly

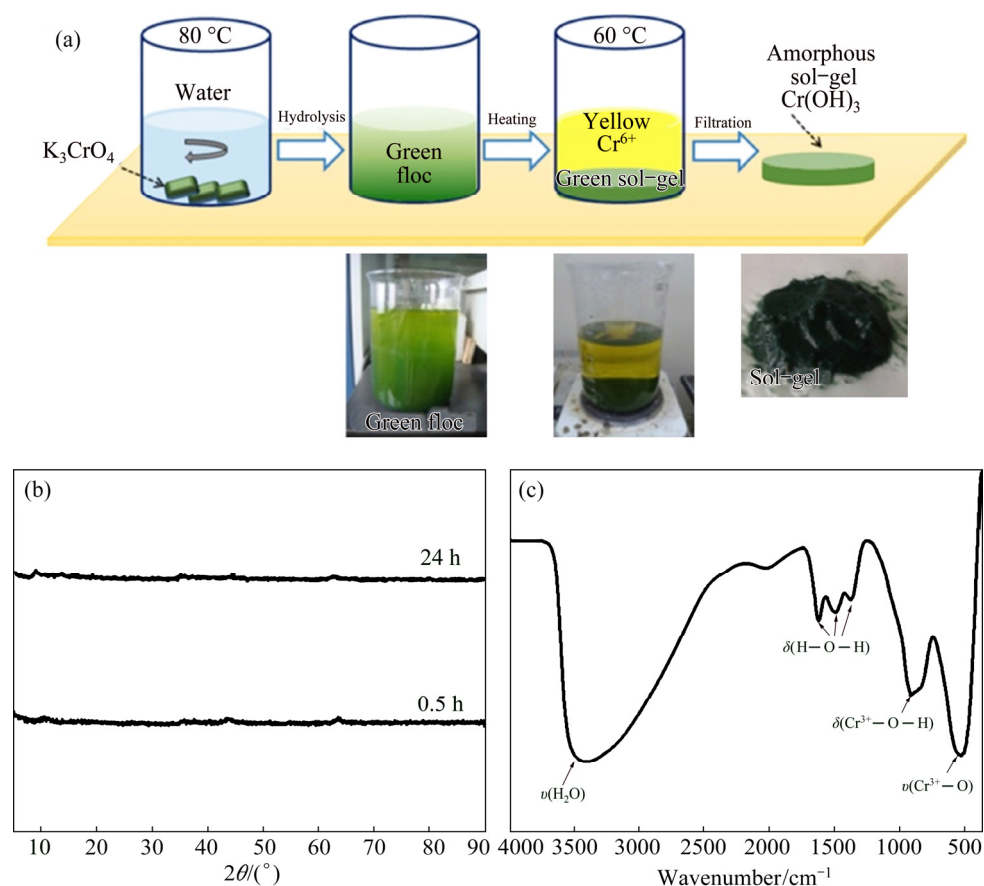


**Fig. 5** Schematic diagram of hydrolysis process of  $K_3CrO_4$  and photos of green flocculent solution and green sol-gel precipitate (a), XRD patterns of hydrolysis products treated at  $80\text{ }^\circ\text{C}$  for 0.5 and 24 h (b) and FT-IR spectrum of hydrolysates (c)

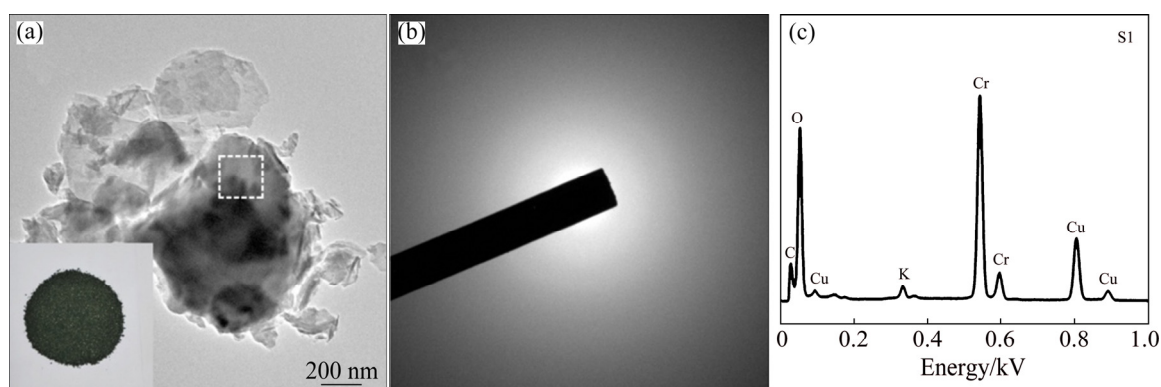


**Fig. 6** TEM image (a), SAED pattern (b) and EDX mapping (c) of hydrolysates (The location of the examined area of SAED pattern and EDX mapping was indicated with a frame. The region in the inset of graph (a) showed the photographs of the  $\text{Cr}(\text{OH})_3$ )

supported the view that  $\text{Cr}(\text{OH})_3$  product was amorphous. Energy dispersive spectroscopy (EDS) was performed to further confirm the composition of the prepared product. The corresponding EDS spectrum highlighted the presence of only chromium, oxygen, and potassium peaks. Besides, Cu and C could also be observed, which was attributed to the copper TEM sample copper grids and carbon film.

#### 4 Discussion

This experimental results discussed above confirmed that the formation of unique large hexagonal crystal may be attributed to the presence of  $\text{KCrO}_2$  with a rhombohedral crystal structure. The results of XRD, FT-IR and SEM analysis were used to explore the hydrolysis mechanism of  $\text{KCrO}_2$ . It could be seen from the XRD and FT-IR results that the peak position of  $\text{KCrO}_2$  disappeared after hydrolysis, and the peak position of  $\text{CrOOH}$  appeared. Generally, the formation of  $\alpha\text{-CrOOH}$  resulted from the decomposition of  $\text{KCrO}_2$ . The possible hydrolysis reaction of the overall process was given as

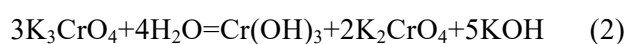


Compared with the former hydrothermal method, this novel intrinsic hydrolysis approach has many preponderance for the preparation of  $\alpha\text{-CrOOH}$ . The hydrolysis treatment is very facile.  $\text{KCrO}_2$  could thoroughly hydrolyze just though slightly extending hydrolysis duration and increasing the temperature ( $80\text{ }^\circ\text{C}$ , 24 h), which avoided other complicated adjusting

processes.

In a recent review, BAMBERGER et al [36] reported that  $\text{K}_3\text{CrO}_4$  reacted with water to form hydrosoluble  $\text{Cr}^{3+}$ , potassium chromate ( $\text{K}_2\text{CrO}_4$ ) and potassium hydroxide (KOH). After boiling for approximately 8 min, the hydrosoluble  $\text{Cr}^{3+}$  formed a solid residue of amorphous chromic hydroxide ( $\text{Cr}(\text{OH})_3$ ). JOHNSON et al [37] determined that the reaction of  $\text{K}_3\text{CrO}_4$  with aqueous acid at  $25\text{ }^\circ\text{C}$  led to solutions with two-thirds chromium in the hexavalent oxidation state and one-third chromium in the trivalent oxidation state. More recently, by measuring UV–Vis absorption and back-titrated  $\text{CrO}_4^{3-}$ , BAILEY et al [38] have reported that a fused solution of  $\text{CrO}_4^{3-}$  was rapidly oxidized to  $\text{CrO}_4^{2-}$  in oxygen, and a solution of  $\text{CrO}_4^{3-}$  in potassium hydroxide was quickly and disproportionately converted into  $2\text{Cr}^{6+}$  and  $\text{Cr}^{3+}$ .

The experimental results of the hydrolysis of  $\text{K}_3\text{CrO}_4$  in this work could be indexed as  $\text{Cr}(\text{OH})_3$  and  $\text{K}_3\text{CrO}_4$ , which was consistent with the previous reported result. In air,  $\text{K}_3\text{CrO}_4$  reacted with water vapor to form two-thirds of  $\text{K}_2\text{CrO}_4$  ( $\text{Cr}^{6+}$ ) and one-third of  $\text{Cr}(\text{OH})_3$  ( $\text{Cr}^{3+}$ ). As previously discussed, the peak position of  $\text{K}_2\text{CrO}_4$  can be obtained from XRD data, which proved the formation of  $\text{K}_2\text{CrO}_4$ . At the same time, the formation of  $\text{Cr}(\text{OH})_3$  could be proved from FT-IR data and product morphology. As a result, after exposing  $\text{K}_3\text{CrO}_4$  in air, one of the product had a XRD phase of  $\text{K}_2\text{CrO}_4$ , and  $\text{Cr}(\text{OH})_3$  was amorphous or had poor crystallinity. The possible hydrolysis reaction of  $\text{K}_3\text{CrO}_4$  was



## 5 Conclusions

(1) The obtained  $\alpha$ -CrOOH was crystallographically pure, and it was identified with a hexagonal plate-like morphology with a grain size of 10  $\mu\text{m}$ .

(2) The prepared amorphous Cr(OH)<sub>3</sub> was identified with lumpy aggregate morphology.

(3) The reaction temperature was only 80 °C and the reaction time was 24 h. In addition, increasing the hydrolysis duration during the crystallization was helpful to increasing the product purity.

(4) This process would be a better alternative for producing Cr(OH)<sub>3</sub> and CrOOH compounds due to its easier implementation and higher flexibility.

## References

- [1] KNAAK J F.  $\gamma$ -CrOOH fluorination catalysts: US Patent, 3992325 [P]. 1976–11–16.
- [2] ADBELSADEK M S, BABU S M. A controlled approach for synthesizing CdTe@CrOOH (core-shell) composite nanoparticles [J]. *Current Applied Physics*, 2011, 11: 926–932.
- [3] HUANG Zhong-lin, CHEN Chang-guo, XIE Ji-yun, WANG Zeng-xiang. The evolution of dehydration and thermal decomposition of nanocrystalline and amorphous chromium hydroxide [J]. *Journal of Analytical and Applied Pyrolysis*, 2016, 118: 225–230.
- [4] SU Chang-qing, LI Li-qing, YANG Zhi-hui, CHAI Li-yuan, LIAO qi, SHI Yan, LI Jia-wei. Cr(VI) reduction in chromium-contaminated soil by indigenous microorganisms under aerobic condition [J]. *Transactions of Nonferrous Metals Society of China*, 2019, 29: 1304–1311.
- [5] HU Jin, MENG De-long, LIU Xue-duan, LIANG Yi-li, YIN Hua-qun, LIU Hong-wei. Response of soil fungal community to long-term chromium contamination [J]. *Transactions of Nonferrous Metals Society of China*, 2018, 28: 1838–1846.
- [6] PARDO P, CALATAYUD J M, ALARCON J. Chromium oxide nanoparticles with controlled size prepared from hydrothermal chromium oxyhydroxide precursors [J]. *Ceramics International*, 2017, 43: 2756–2764.
- [7] MAHMOUD H R. Novel mesoporous Gd<sup>3+</sup> doped Cr<sub>2</sub>O<sub>3</sub> nanomaterials: Synthesis, characterization, catalytic and antitumor applications [J]. *Advanced Powder Technology*, 2016, 27: 1446–1452.
- [8] SANGEETHA S, BASHA R, SREERAM K J, SANGILIMUTHU S N, UNNI NAIR B. Functional pigments from chromium(III) oxide nanoparticles [J]. *Dyes and Pigments*, 2012, 94: 548–552.
- [9] LIANG Shu-ting, ZHANG Hong-ling, LUO Min-ting, LUO Ke-jun, LI Ping, XU Hong-bin, ZHANG Yi. Colour performance investigation of a Cr<sub>2</sub>O<sub>3</sub> green pigment prepared via the thermal decomposition of CrOOH [J]. *Ceramics International*, 2014, 40: 4367–4373.
- [10] WEI Guang-ye, QU Jing-kui, YU Zhi-hui, LI Yong-li, GUO Qiang, QI Tao. Mineralizer effects on the synthesis of amorphous chromium hydroxide and chromium oxide green pigment using hydrothermal reduction method [J]. *Dyes and Pigments*, 2015, 113: 487–495.
- [11] LI Zhong-fu, DU Yi, CHEN Zhong-tao, SUN Dan-dan, ZHU Chao-feng. Synthesis and characterization of cobalt doped green ceramic pigment from tannery sludge [J]. *Ceramics International*, 2015, 41: 12693–12699.
- [12] POLANSKI M, BYSTRZYCKI J, VARIN R A, PLOCINSKI T, PISAREK M. The effect of chromium (III) oxide (Cr<sub>2</sub>O<sub>3</sub>) nanopowder on the microstructure and cyclic hydrogen storage behavior of magnesium hydride (MgH<sub>2</sub>) [J]. *Journal of Alloys and Compounds*, 2011, 509: 2386–2391.
- [13] SURYAWANSHI D N, PATIL D R, PATIL L A. Fe<sub>2</sub>O<sub>3</sub>-activated Cr<sub>2</sub>O<sub>3</sub> thick films as temperature dependent gas sensors [J]. *Sensors and Actuators B: Chemical*, 2008, 134: 579–584.
- [14] ABBAS S M, AHMAD N, ATA UR R, RANA U A, KHAN S U D, HUSSAIN S, NAM K W. High rate capability and long cycle stability of Cr<sub>2</sub>O<sub>3</sub> anode with CNTs for lithium ion batteries [J]. *Electrochimica Acta*, 2016, 212: 260–269.
- [15] MARUTHAPANDIAN V, MURALIDHARAN S, SARASWATHY V. Liquid-free alkaline gel filled reference electrode based on Cr<sub>2</sub>O<sub>3</sub> spheres [J]. *Indian Journal of Chemistry A*, 2015, 54: 1215–1220.
- [16] ZHANG Xiao-yu, CHEN Ya-jie, LI Zhen-ya. Large magnetocaloric effect in chromium dioxide with second-order phase transition [J]. *Journal of Physics D: Applied Physics*, 2007, 40: 3243–3247.
- [17] BELEVTSSEV B, DALAKOVA N, OSMOLOWSKY M, BELIAYEV E Y, SELUTIN A. Transport and magnetotransport properties of cold-pressed CrO<sub>2</sub> powder, prepared by hydrothermal synthesis [J]. *Journal of Alloys and Compounds*, 2009, 479: 11–16.
- [18] PEI Zhen-zhao, XU Hong-bin, ZHANG Yi. Preparation of CrO<sub>2</sub> nanoparticles via oxidation method [J]. *Materials Letters*, 2012, 76: 205–207.
- [19] LAUBENGAYER A W, MCCUNE H W. New crystalline phases in the system chromium(III) oxide–water [J]. *Journal of the American Chemical Society*, 1952, 74: 2362–2364.
- [20] CHRISTENSEN A N. Hydrothermal preparation and magnetic-properties of Alpha-CrOOH, Beta-CrOOH, and Gamma-CrOOH [J]. *Acta Chemica Scandinavica A — Physical and Inorganic Chemistry*, 1976, 30: 133–136.
- [21] CHRISTEN A N. Crystal structure of a new polymorph of CrOOH [J]. *Inorganic Chemistry*, 1966, 5: 1452–1453.
- [22] HAMILTON W C, IBERS J A. Structures of HCrO<sub>2</sub> and DCrO<sub>2</sub> [J]. *Acta Crystallographica*, 1963, 16: 1209–1212.
- [23] YANG Jing, MARTENS W N, FROST R L. Transition of chromium oxyhydroxide nanomaterials to chromium oxide: A hot-stage Raman spectroscopic study [J]. *Journal of Raman Spectroscopy*, 2010, 42: 1142–1146.
- [24] KITAKA S, TAHARA T. Thermal decomposition of chromium oxide hydroxide: II. Texture change of  $\alpha$ -HCrO<sub>2</sub> through thermal decomposition under vacuum [J]. *Journal of*

- Colloid and Interface Science, 1986, 112: 252–260.
- [25] KITAKA S, FUJINAGA R, MORISHIGE K, MORIMOTO T. Adsorption of water on the surfaces of  $\alpha$ -HCrO<sub>2</sub> and Cr<sub>2</sub>O<sub>3</sub> [J]. Journal of Colloid and Interface Science, 1984, 102: 453–461.
- [26] YANG Jing, BAKER A, LIU Hong-wei, MARTENS W, FROST R. Size-controllable synthesis of chromium oxyhydroxide nanomaterials using a soft chemical hydrothermal route [J]. Journal of Materials Science, 2010, 45: 6574–6585.
- [27] ALI N Z, NUSS J, JANSEN M. A new polymorph of potassium chromate(III),  $\beta$ -KCrO<sub>2</sub>, and reinvestigation of  $\alpha$ -KCrO<sub>2</sub> [J]. Journal of Inorganic and General Chemistry, 2013, 639: 241–245.
- [28] DELMAS C, DEVALETTE M, FOUASSIER C, HAGENMULLER P. Les phases K<sub>x</sub>CrO<sub>2</sub> (X≤1) [J]. Materials Research Bulletin, 1975, 10: 393–398.
- [29] LI Ping, XU Hong-bin, ZHENG Shi-li, ZHANG Yi, LI Zuo-hu, BAI Yu-lan. A green process to prepare chromic oxide green pigment [J]. Environmental Science & Technology, 2008, 42: 7231–7235.
- [30] BAI Yu-lan, XU Hong-bin, ZHANG Yi, LI Zuo-hu. Reductive conversion of hexavalent chromium in the preparation of ultra-fine chromia powder [J]. Journal of Physics and Chemistry of Solids, 2006, 67: 2589–2595.
- [31] RATNASAMY P, LEONARD A J. Structural evolution of chromia [J]. The Journal of Physical Chemistry, 1972, 76: 1838–1843.
- [32] PEI Zhen-zhao, XU Hong-bin, ZHANG Yi. Preparation of Cr<sub>2</sub>O<sub>3</sub> nanoparticles via C<sub>2</sub>H<sub>5</sub>OH hydrothermal reduction [J]. Journal of Alloys and Compounds, 2009, 468: L5–L8.
- [33] DOUGLASS R M. The crystal structure of HCrO<sub>2</sub> [J]. Acta Crystallographica, 1957, 10: 423–427.
- [34] YAO Zhi-mao, LI Zuo-hu, ZHANG Yi. Studies on thermal dehydration of hydrated chromic oxide [J]. Journal of Colloid and Interface Science, 2003, 266: 382–387.
- [35] SNYDER R G, IBERS J A. O—H—O and O—D—O potential energy curves for chromous acid [J]. The Journal of Chemical Physics, 1962, 36: 1356–1360.
- [36] BAMBERGER C E, DONALD M, RICHARDSON D M. Chemical cycle for thermochemical production of hydrogen from water: US Patent, 3927192 [P]. 1975–12–16.
- [37] JOHNSON L H, HEPLER L G, BAMBERGER C E, RICHARDSON D M. The enthalpy of formation of potassium chromate(V), K<sub>3</sub>CrO<sub>4</sub>(c) [J]. Canadian Journal of Chemistry, 2011, 56: 446–449.
- [38] BAILEY N, SYMONS M C R. Structure and reactivity of the oxyanions of transition metals. Part III. The hypochromate ion [J]. Journal of the Chemical Society, 1957, 1: 203–207.

## 通过 K<sub>x</sub>CrO<sub>y</sub> 便捷水解制备六方和无定型羟基氧化铬

梁书婷<sup>1,2</sup>, 张红玲<sup>3,4</sup>, 徐红彬<sup>3,4</sup>

1. 重庆文理学院 化学与环境工程学院, 重庆 402160;
2. 重庆文理学院 环境材料与修复技术重庆市重点实验室, 重庆 402160;
3. 中国科学院 过程工程研究所 湿法冶金清洁生产国家工程实验室, 北京 100190;
4. 中国科学院 过程工程研究所 绿色过程与工程重点实验室, 北京 100190

**摘要:** 系统研究 KCrO<sub>2</sub> 和 K<sub>3</sub>CrO<sub>4</sub> 的水解过程和机理。XRD、IR 和 SEM 的表征结果表明, 在 80 °C 的低反应温度和 24 h 的反应时间下, 可以实现水解反应。此外, 通过水解单相六方 KCrO<sub>2</sub>, 能形成灰绿色六方片状直径为 10 μm 的  $\alpha$ -CrOOH; 而通过水解立方 K<sub>3</sub>CrO<sub>4</sub>, 能形成绿色无定形团聚体形态 Cr(OH)<sub>3</sub> 溶胶凝胶。通过上述水解反应合成纯相羟基氧化铬是一种非常简便与快速的方法。

**关键词:** 水解过程; CrOOH; 氧化铬; 活性 K<sub>x</sub>CrO<sub>y</sub>; 反应机理

(Edited by Xiang-qun LI)